

ABSTRACT

Using Remote Sensing to Assess Potential Impacts of Hurricanes on Mosquito Habitat Formation: Investigating the Mechanisms for Interrelationship between Climate and the Incidence of Vector-Borne Diseases

Zainab R. Naqvi, M.S.

Mentor: Joseph D. White, Ph.D.

The present study examined the relationship between climate and the incidence of vector-borne disease. The climatological phenomenon El Niño Southern Oscillation (ENSO) was found to be significant in predicting the frequency and intensity of hurricane seasons for the Atlantic Ocean and the Yucatan Peninsula between 1985 to 2007. Satellite analysis for hurricanes that impacted the Yucatan Peninsula, specifically the country of Belize, between 1995 and 2007 determined changes in the Normalized Difference Vegetation Index (NDVI), mid-infrared range (MIR), and thermal infrared range (TIR) immediately after and one month after the hurricanes. Regression analyses found that correlations between reported cases of malaria and dengue fever for Belize and changes in the NDVI, MIR, and TIR existed between immediate and persistent impacts and disease incidence.

Using Remote Sensing to Assess Potential Impacts of Hurricanes on Mosquito Habitat
Formation: Investigating the Mechanisms for Interrelationship Between Climate and the
Incidence of Vector-Borne Diseases

by

Zainab Raza Naqvi, B.S.

A Thesis

Approved by the Department of Environmental Studies

Susan P. Bratton, Ph.D., Chairperson

Submitted to the Graduate Faculty of
Baylor University in Partial Fulfillment of the
Requirements for the Degree
of
Masters of Science

Approved by the Thesis Committee

Joseph D. White, Ph.D., Chairperson

Sara E. Alexander, Ph.D.

Richard E. Duhrkopf, Ph.D

Accepted by the Graduate School
December 2009

J. Larry Lyon, Ph.D., Dean

Copyright © 2009 by Zainab R. Naqvi

All rights reserved

TABLE OF CONTENTS

List of Figures	v
List of Tables	vi
Acknowledgments	vi
Chapter One	
Introduction	1
Belize	3
Hurricanes	8
El Niño Southern Oscillation	10
Vector-Borne Diseases	12
Remote Sensing	15
Chapter Two	
Methods	18
El Niño Southern Oscillation and hurricane activity	18
Hurricane impacts through satellite analysis	21
Disease and satellite analysis	26
Chapter Three	
Results	31
El Niño Southern Oscillation and hurricane activity	31
Hurricane impacts through satellite analysis	32
Disease and satellite analysis	35

Chapter Four	
Discussion	40
El Niño Southern Oscillation and hurricane activity	40
Hurricane impacts through satellite analysis	42
Disease and satellite analysis	44
Chapter Five	
Conclusions	50
References	52

LIST OF FIGURES

Figure 1. Map of Belize districts	4
Figure 2. Land use and land cover map for mainland Belize, 1989/1992	6
Figure 3. Distribution of Atlantic storm frequency against Southern Oscillation Index (SOI) values	20
Figure 4. Distribution of Yucatan storm frequency against Southern Oscillation Index (SOI) values	21
Figure 5. Percent change calculations for the Normalized Difference Vegetation Index (NDVI)	33
Figure 6. Percent change calculations for mid-infrared (MIR) reflectance	34
Figure 7. Percent change calculations for thermal infrared (TIR) emittance	34

LIST OF TABLES

Table 1. Average annual rainfall in Belize	4
Table 2. Mean annual temperature in Belize	4
Table 3. Land use in Belize, 1995 and 2005	5
Table 4. Belize population by district in 2000	8
Table 5. Belize hurricane history	9
Table 6. Spectral extent of Landsat-5 satellite	22
Table 7. Spectral extent of Landsat-7 satellite	23
Table 8. Record of satellite imagery download	25
Table 9. Number of malaria and dengue cases by year for Belize	28
Table 10. Number of malaria cases by district for Belize by year	28
Table 11. Number of dengue cases by district for Belize by year	28
Table 12. Mann Whitney U test results for storms and hurricane frequency and intensity	32
Table 13. Mean differences in percent change calculations in NDVI, MIR, and TIR	32
Table 14. Stepwise linear regression model results between malaria in Belize to percent changes in NDVI	35
Table 15. ANOVA results from the stepwise linear regression of malaria and percent change in NDVI	35
Table 16. Stepwise linear regression model results between dengue fever in Belize to percent changes in TIR	36
Table 17. ANOVA results from the stepwise linear regression of dengue fever and percent change in TIR	36

Table 18. Pearson correlation results between incidence of malaria and percent changes in the NDVI for districts Belize, Stann Creek, and Toledo	37
Table 19. Pearson correlation results between incidence of malaria and percent changes in the mid-infrared (MIR) reflectance for districts Belize, Stann Creek, and Toledo	37
Table 20. Pearson correlation results between incidence of malaria and percent changes in the thermal (TIR) emittance for districts Belize, Stann Creek, and Toledo	37
Table 21. Pearson correlation results between incidence of dengue fever and percent changes in the NDVI for districts Belize, Stann Creek, and Toledo	38
Table 22. Pearson correlation results between incidence of dengue fever and percent changes in the mid-infrared (MIR) reflectance for districts Belize, Stann Creek, and Toledo	38
Table 23. Pearson correlation results between incidence of dengue fever and percent changes in the thermal infrared (TIR) emittance for districts Belize, Stann Creek, and Toledo	38
Table 24. Percentage of population in Belize with access to sewage systems, by district	47

ACKNOWLEDGMENTS

First and foremost, I would like to acknowledge my advisor, Dr. Joseph White. Without him this thesis would be a shell of its self. His supreme patience, knowledge, and assistance in the planning, execution, and completion of this research were all vital to the completion of the project. I would also like to thank Dr. Sara Alexander for allowing me the opportunity to study in a country as wonderful as Belize. Finally, I'd like to thank Dr. Richard Duhrkopf for his assistance and knowledge.

I would also like to thank the various ministries and agencies within the Government of Belize that have helped me assimilate the data necessary to complete this research. This includes, but is not limited to, the Ministry of Health, the Ministry of Agriculture, and the Central Statistics Office, who were all helpful in providing me with information that I needed.

I would also like to acknowledge the C. Gus Glasscock, Jr. Endowed Fund for Excellence in Environmental Sciences and the National Oceanic and Atmospheric Administration, without whose funding this research would not have been possible.

I would also like to thank my friends, for supporting me in this venture, especially since it so often vacillates between nonsensical and ideal to those who know me best. Without them, and reassurances they provided during the many 2am panic phone calls, this thesis might not have been completed.

And lastly, I'd like to thank The Moms and The Dad, Bhaiya, and Masaji for being there.

CHAPTER ONE

Introduction

Climate variability has had a demonstrated impact on infectious diseases (Epstein 2002, 374). ENSO-driven climate changes have been linked to increased disease transmission (Epstein 2001, 758; Pascual et al. 2000, 1766; Epstein 1999, 347; Checkley et al. 1997, 442). Mosquitoes, as poikilotherms, are very sensitive to temperature changes, with warming events causing increases in reproduction and the number of blood meals taken, a longer reproductive season, and a shorter maturation period for pathogens (Epstein 2005, 1435).

Extremes in climactic condition can have effects on vector abundance in different ways, which can increase the risk of outbreaks of various infectious diseases (Epstein 2002, 373-74). Drought conditions can suppress mosquito predators (Bouma and Dye 1997, 1772). On the other hand, heavy rains can increase food supplies, which can promote the likelihood of good conditions for mosquito breeding and propagation (Linthicum et al. 1999, 397). There is a higher risk of malaria due to elevated *Anopheles* spp. populations from the flooding of immature habitats following periods of heavy rainfall (Gabaldon 1949, 113). Various studies of the transmission of malaria in highland areas have suggested that temperature is a principal limiting factor in the epidemiology of malaria (Haworth 1988, 1379-420; Macdonald 1957). Higher temperatures can possibly assist malaria transmission by shortening the extrinsic cycle of the *Plasmodium* in the vector (Pulwarty 1994).

Habitat specificity of *Anopheles* spp. and *Aedes* spp. mosquitoes allow for estimation and prediction of where outbreaks are likely to occur. For example, the southern and western portions of the tropical country of Belize have more broadleaf hill forests, agricultural land, and wetland vegetation types, and have consistently higher rates of malaria than northern urbanized areas (Hakre et al. 2004). Anthropogenic changes through the conversion of forest land to agricultural land has also had an impact on mosquito populations, as agricultural runoff has contributed to providing habitats for mosquito vectors (Grieco et al. 2006, 615). By studying the dynamics of spatial heterogeneity, interactions among heterogeneous landscapes, and effects of these interactions on biotic processes, we can better understand mosquito dispersion and habitat prevalence (Kitron 1998, 435-38). Changes in land-use maps over time can provide information about the developmental changes in the landscape which could be contributing factors to disease.

The goal of this study was to determine whether climate was the major driver of vector-borne diseases, specifically malaria and dengue fever, within the country of Belize since 1985. In order to determine these relationships, the study was separated into different questions, each addressing an integral part of the larger picture. Specifically, the following general questions are addressed by the hypotheses presented within this work:

What was the impact of climate on hurricane activity in the Atlantic?

What measurable impacts did hurricane activity have on land cover and water cover within the country of Belize?

How would land cover changes likely affect vectors, and the diseases that they vector?

What confounding factors contribute to variations in vector-borne disease occurrence that are not explained by climate changes alone?

In order to achieve these goals, I will target a few objectives for each component of the study. The first objective is to understand the influence that the El Niño Southern Oscillation exerts on the Atlantic hurricane season, in order to determine the role that large-scale climate shifts may have on hurricane activity. The next objective is to determine what measurable impacts hurricane activity has on land and vegetative cover, and water deposition, within the country of Belize. The third objective is to determine how vegetation cover changes, and predicted areas of water inundation, correspond to the incidence of vector-borne diseases, specifically malaria and dengue fever, in Belize.

Belize

Belize is located in Central America, between Mexico and Guatemala adjacent to the Caribbean Sea and covers 22,966 square kilometers (15°45'-18°30'N and 87°30'-89°15'W on UTM Zone 16; Central Statistics Office 2004). The country is divided into six political districts: Corozal, Orange Walk, Belize, Cayo, Stann Creek, and Toledo (Fig. 1; Statistical Institute of Belize 2008). The topography is described as mostly flat, with swampy coastal plains and the Maya Mountain foothills in the south that extend westward into Guatemala.



Figure 1. District-based map of Belize

The climate of Belize is tropical, with wet and dry seasons (Land and Surveys Department 2006). Average annual rainfall is variable, ranging from around 1,700 mm to over 2,100 mm (Table 1).

Table 1. Average annual rainfall in Belize, 2001-2005

Year	Average Annual Rainfall (mm)
2001	1,994
2002	1,761
2003	1,692
2004	1,754
2005	2,134

Source: National Meteorological Services, 2006

Mean annual temperature is moderately variable, expected for a tropical climate, with annual minimum and maximum temperatures of 22°C and 31°C, respectively (Table 2).

The country is a mixture of different types of land cover and land uses (Fig. 2). Ecosystems described for Belize include urban areas, agricultural lands, wetlands,

savannahs, and forested wooded areas, which includes broadleaf forests, pine forests, and mangrove and littoral forests that are represented in all political districts.

Table 2. Mean annual temperature in Belize, 1970-2003

Year	Max	Min	Average
1970-1997	30°C	23°C	27°C
1998	31°C	24°C	27°C
1999	30°C	22°C	26°C
2000	30°C	23°C	27°C
2001	30°C	23°C	27°C
2002	31°C	23°C	27°C
2003	31°C	23°C	27°C

Source: Meteorology Department, 2006

The most current assessments of land cover are based on measurements by the Land Information Center (LIC) of Belize. In 2005, the majority of the land fell under “allocated lands,” which includes lands devoted to agriculture, followed by “protected land,” including federally-controlled areas (Table 3).

Table 3. Land use in Belize 1995 and 2005

Type of land	1995 (km)	2005 (km)
Protected land	8,013	7,998
Allocated land	11,093	12,546
Urban land	38	130
Unallocated land	3,821	2,291
Total land area	22,965	22,965

Source: Land and Surveys Department, 2006

A study conducted by Hakre et al. in 2004 found that areas with highest malaria rates were those with a higher total area of agricultural land, broadleaf forests, and seasonally waterlogged fire-induced shrubland, while areas with lower malaria rates were those with higher total area of mangrove forests, needle-leaf forests, seasonal swamp

forests, tall herb wetland communities, urban development, and water. Southern Belize also has more broadleaf hill forests, extensive river systems, and gets more annual precipitation than northern Belize. The northern half of Belize is mainly flat, low-lying coastal plains and a low plateau. In the south, there is a narrow coastal plain, with the Maya Mountains and a tall plateau in the west (Waddell 1961, 57-58).

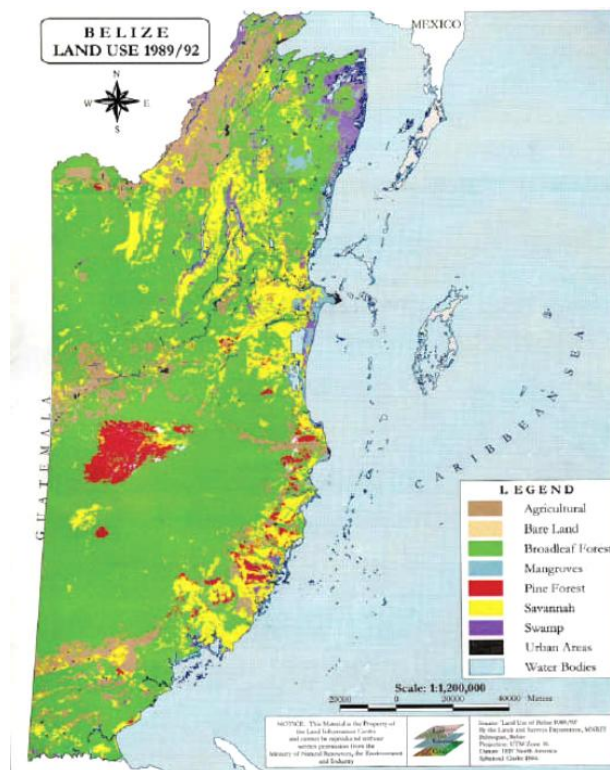


Figure 2. Land use and land cover map for mainland Belize, 1989/1992

Previous land cover assessments by the LIC also provide a history of the trend of land cover changes in the country. The most evident trend is the increase in lands used for urban development with a concomitant decrease in lands that are considered “protected.” Changes in land cover type have been shown to have an impact on the incidence of vector-borne diseases (Chaves et al. 2008; Lindblade et al. 2000, 272).

Deforestation of land and conversion to agriculture, and increased population migrations to these areas all play a role in increasing the incidence of mosquito-borne diseases (Guerra et al. 2006, 189-90).

There is increased pressure on natural resources in Belize. Changes in land cover types in Belize are associated with recent increased population size, increased urban development, increased conversion to agricultural lands, and increased ecotourism promotion. The increase in population size was the result of both a high population growth rate and increased immigration into the country from Mexico and Guatemala. As a result of increasing populations, there is a need for urban development to accommodate the growing urban population. Increases in agricultural lands (allocated lands) also reflect the increased population, as a result of increased demand for agricultural products. Rural areas also have a high degree of poverty, and poor rural communities also engage in farming and exploitation of forest resources to a greater extent than urban areas. The result is an increase in pressure on resources, which means more land clearing and changes in land use. However, the growth of ecotourism as an industry has had a hand in promoting the protection of natural reserves and other protected natural areas, which is reflected in the limited loss of protected areas over time.

Current government regulations and policies in place have attempted to limit environmental degradation and loss of biodiversity. As of 2003, twenty-two Acts were in place with multiple regulations directly relating to impacts on biological diversity (National Policy Development Committee 2003, 14). However, continued environmental degradation has been the result of lack of enforcement of legislation. Another problem is

the overlap of legal mandates between different agencies over managing the same resource, resulting in poor coordination and implementation of existing legislation.

Three important districts to consider within the country of Belize are Belize, Stann Creek, and Toledo. These three districts are all coastal districts, and therefore likely to demonstrate physical changes from hurricane impacts. They also all have varying degrees of urban development (Table 4). Belize District has the highest relative urban population, with cities like Belize City and San Pedro. Stann Creek District has recently increased development, with developing towns such as Placencia and Dangriga, although it has not yet reached the level of Belize District. Toledo District, comprised of small towns and villages such as Punta Gorda, has had very little urban development, with most of its population living rurally.

Table 4. Population of Belize by district separated by urban and rural areas in 2000

Population type	Population	Percent
Country		
Urban	108,602	46.79
Rural	123,509	53.21
Total	232,111	100
Belize		
Urban	49,392	78.32
Rural	13,669	21.68
Total	63,061	100
Stann Creek		
Urban	8,424	34.46
Rural	16,019	65.54
Total	24,443	100
Toledo		
Urban	4,266	18.45
Rural	18,851	81.55
Total	23,117	100

Source: Statistical Institute of Belize, 2008

Hurricanes

Hurricanes occur most frequently around the equator during the late summer and early fall. In the North Atlantic and the Caribbean, the official hurricane season is from June 1 to November 30. Hurricanes typically form under three conditions: a sea surface temperature at or above 26°C, high humidity, and high wind speeds (Hood 1998, 19-21). Low pressure drives wind speeds to accelerate, increasing the size and power of the hurricane (Treaster 2007, 17-19). Hurricane categories are typically based on the Saffir-Simpson scale. Over the past ten to fifteen years, catastrophic hurricanes have affected Belize, particularly in 1998, 2000, 2001, and 2005. For this study, years in which hurricanes made landfall in Belize were the focal point of study and analysis (Table 5).

Table 5. Belize Hurricane History

Year	Name	Dates of persistence
1995	Opal	Sept. 27-Oct. 6
	Roxanne	Oct. 7-21
1996	Dolly	Aug 19-25
1998	Mitch	Oct. 22-Nov. 9
1999	Tropical Storm Katrina	Oct. 28-Nov 1
2000	Gordon	Sept. 14-21
	Keith	Sept. 28-Oct. 6
2001	Chantal	Aug 14-22
	Iris	Oct. 4-9
2003	Tropical Storm Bill	June 28-July 3
	Claudette	July 7-17
	Tropical Storm Larry	Sept. 27-Oct 7
2005	Cindy	July 3-11
	Emily	July 11-21
	Stan	Oct. 1-5
	Wilma	Oct. 15-26
2007	Dean	Aug. 13-23
	Felix	Aug. 31-Sept. 6

Source: Unisys Weather, 2007

Short-term impacts of hurricanes include damage caused by winds, flooding, and storm surges. High speed winds can destroy buildings and force rain and seawater across larger areas. Aside from winds, hurricanes can bring anywhere from 150 to 305 mm of rain in a single day. Ocean levels can rise 30 to 70 cm higher than the average high tide, causing a storm surge which increases flooding and pushes water further inland (Treaster 2007, 20-21; Hood 1998, 25-29). Increased rainfall can result in increased shallow and deep freshwater pools that serve as breeding sites for mosquitoes. Long-term impacts of hurricanes include retained water pools as breeding sites and the increased reservoir of disease within animal and human populations due to initial vector and disease outbreaks caused by hurricane effects.

El Niño Southern Oscillation

The El Niño Southern Oscillation (ENSO) is a climatological phenomenon that occurs in an irregular cycle of every 2-7 years. The term “El Niño” refers to the large-scale ocean-atmosphere interactions that cause periodic warming in sea surface temperatures across the central and east-central equatorial Pacific, marking the warm phase of the ENSO (Anyamba et al. 2006). The opposite cold phase of the ENSO is known as La Niña. The ENSO is a source of inter-annual variability in weather and climate around the world. El Niño and La Niña are officially defined as “sustained sea surface temperature anomalies,” and can cause localized impacts such as flooding and droughts through drastically increased or decreased rain activity (Anyamba et al. 2006).

ENSO is the result of changes in the equatorial trade winds in the Pacific Ocean, which then causes changes in the equatorial Pacific surface ocean circulation. The variations in the trade winds and ocean circulation cause changes in the sea surface

temperature, which then feeds back into the atmosphere, causing more changes to the surface winds. This cyclical atmosphere-ocean interaction continues to build until a large shift in warm waters occurs across the Pacific towards the South American coast. During an El Niño event, sea surface temperatures can increase by as much as 2-4°C. Changes in atmospheric circulation cause changes in precipitation, with increased rainfall on western South American coast, and drier conditions in the Caribbean and northern Brazil (Steffan et al. 2005, 60-61). El Niño events usually act to reduce hurricane activity in the Caribbean Sea region by increasing vertical wind shear (Anyamba et al. 2006). The opposite occurs during a La Niña event.

Two parameters of the El Niño Southern Oscillation are anomalies of the sea surface temperatures in the eastern equatorial Pacific and the Southern Oscillation Index (SOI). The Southern Oscillation Index is measured as air pressure deviations between the eastern and western Pacific, taken from the island of Tahiti and Darwin, Australia (Bouma and van der Kaay 1996, 89). An El Niño shows a positive deviation of the sea surface temperature and a negative deviation of the SOI, while the La Niña events show a negative deviation from the sea surface temperature and a positive deviation of the SOI (Bouma and van der Kaay 1996, 89; Nicholls 1993). The SOI is the most commonly used index to measure the ENSO phenomenon (Glantz, Katz, and Nicholls 1991, 1-12; Chagas and Puppi 1986, 1-15).

Extremes in climate conditions can affect the numbers of mosquito vectors. A strong El Niño event can cause droughts through reduced hurricane activity and rain, which can suppress mosquito predators, leading to increased disease transmission (Anyamba et al. 2006). On the other side, a strong La Niña event can cause increased

hurricane activity which can increase rainfall and breeding habitats for mosquitoes. Several disease outbreaks have been linked to El Niño, including Murray Valley encephalitis, bluetongue, Ross River virus disease, dengue fever, and malaria (Woodruff 2002, 385-90; Nicholls 1993, 1284-85; Nicholls 1986, 587-88). Finally, the impact of the ENSO on hurricane activity in the Caribbean has become increasingly important as increased global temperatures cause higher extremes in the SOI and in sea surface temperatures.

Vector-Borne Diseases

Vector-borne diseases are diseases that are caused by pathogens that are carried and transmitted by arthropod vectors. For the cases of this study, all vectors associated with vector-borne diseases are mosquitoes. Mosquitoes are responsible for vectoring several important pathogens to disease, including *Plasmodium* spp. (which causes malaria) and the dengue virus (which causes dengue fever and dengue hemorrhagic fever). Mosquitoes play an important medical role in Central America in the spread of these diseases.

Anopheles Mosquitoes and Malaria

Anopheles spp. mosquitoes are vectors for *Plasmodium* spp., the causative agent of malaria. *Anopheles* mosquitoes breed in water, usually permanent or semi-permanent habitats, such as the edges of lakes, ponds, streams, and pools, although they also commonly use irrigated fields and reservoirs as breeding sites (Foster and Walker 2002, 213-22). *Anopheles* mosquitoes are usually found in deciduous and mixed forests, as well as near human habitation (Palsson et al. 2004, 746-52). Female *Anopheles* lay their

eggs in small pools of water (Foster and Walker 2002, 213-22). Important development factors include quantity of water, density of larvae within the pool, and salinity of the water (el-Akad 1992, 459-65). *Anopheles* eggs are laid singly on the surface of the water and increased temperatures accelerate the development of *Anopheles* aquatic larvae (Khasnis and Nettleman 2005, 693). Optimal larval development for *Anopheles* is 28°C and optimal adult development is between 28°C and 32°C (Bayoh and Lindsay 2003, 375-81). *Anopheles* mosquitoes can survive for several weeks in this larval stage.

There are four species of *Plasmodium* that cause malaria: *Plasmodium falciparum*, *Plasmodium vivax*, *Plasmodium malariae*, and *Plasmodium ovale*. *P. falciparum* and *P. vivax* is commonly found in the tropics, with the range of *P. vivax* extending to some temperate areas. *P. malariae* has a wide distribution but is not as common, and *P. ovale* occurs mainly in Africa (Foster and Walker 2002, 240-42). The optimum temperature for development of *Plasmodium falciparum* and *Plasmodium vivax* in a mosquito host is 18°C and 15°C, respectively (Patz and Reisen 2001, 171). *Plasmodium* spp. transmission cannot occur below 16°C or above 33°C, with ideal conditions between 20°C and 30°C with high humidity (Khasnis and Nettleman 2005, 693). At least 20°C is needed to create a malaria epidemic (Lindsay and Martens 1998, 34-35). For example, at 20°C, it takes *P. falciparum* 26 days to incubate; at 25°C, it only takes 13 days to incubate (Bunyavanich et al. 2003, 44-52).

Aedes Mosquitoes and the Dengue Virus

Aedes mosquitoes generally develop in temporary water, with eggs laid on or attached to solid substrates out of water. The larvae remain quiescent until inundated. *Aedes* eggs can survive periods of cold and desiccation and can remain viable for years.

Hatching will occur at warm temperatures after the eggs have been submerged. Preferred habitats for *Aedes* oviposition include floodplains, salt marshes, tree holes, and artificial containers. Aedine species often broadly distribute eggs over several potential development sites, into water containers, and over drying mud or plant debris on low ground. Ideal conditions for *Aedes* larval growth is 26°C to 28°C (Foster and Walker 2002, 213-22).

Female *Aedes* spp. mosquitoes become infected with the dengue viruses following a blood meal from an infected host. During the extrinsic incubation period, which typically lasts from 7 to 10 days, the *Aedes* spp. mosquito is capable of transmitting the viruses. Infected mosquitoes can then transmit the viruses during subsequent blood meals (Yang and Ferreira 2007, 401; Veronesi 1991).

Dengue fever is caused by the dengue virus, a flavivirus that is transmitted by the mosquitoes of the genus *Aedes* spp. (Kurane 2006, 330). As a result of being pathogenic in humans and capable of transmission in heavily population areas, dengue virus can cause widespread epidemics in many tropical and subtropical regions of the world where *Aedes* spp. vectors are found (Monath 1988). There are four different serotypes of dengue virus, and all four serotypes cause three distinct syndromes – classic dengue fever, dengue hemorrhagic fever, and dengue shock syndrome (Yang and Ferreira 2007, 401).

Factors Affecting Vector-borne Diseases

The numbers of mosquito that can serve as vectors of pathogens is affected primarily by the presence of breeding sites for mosquitoes and by the existence of optimal conditions to promote mosquito growth. Breeding sites for mosquitoes can

develop as a result of rainfall which can cause inland flooding in geographically flat or depressed areas. Optimal conditions for mosquito growth include temperatures between 26°-28°C (78°-82°F), water sources for the eggs, larvae, and pupae (which require at least a film of water for most species), and food sources from organic detritus, suspended materials, and small organisms, including bacteria, protists, fungi, algae, and microinvertebrates (Foster and Walker 2002, 213-22).

Remote Sensing

Remote sensing techniques have been applied in the prediction and detection of breeding habitats for mosquitoes (Achee et al. 2006, 382). The use of remotely sensed data to predict areas that are high risk for vector populations is based on the relationship between individual vector species and specific environmental variables, including emergent vegetation, precipitation levels and persistence, and surface water (Andre, Roberts, and Rejmankova 1995, 27-35). Remote sensing can be used to measure biophysical variables including location, elevation, color, chlorophyll absorption characteristics, biomass, temperature, surface texture, and moisture content (Lillesand and Kiefer 1994; Jensen et al. 1989, 111-32). Remote sensing can also be used to identify and map potential parasite, vector and host habitats. These data can be utilized to monitor changes in habitats and predict possible associated changes in vector and host populations and map disease risks used for control programs (Hay 1997, 105-06; Hugh-Jones 1989, 244-51).

Remote sensing capabilities vary with regard to spatial resolution, temporal resolution, and spectral resolution (Kitron 1998, 438). Finer spatial resolution images, like those from Landsat Thematic Mapper (TM), with a spatial resolution of 30 m, and

the French satellite SPOT, with a spatial resolution of 10-20 m, can be used to characterize vector habitats on a finer spatial scale (Lillesand and Kiefer 1994; Kitron and Mannelli 1994, 198-239). Images with lower spatial resolution can be useful for coarser-scale studies of vector distribution. The advanced very high resolution radiometer (AVHRR) images with a spatial resolution of 1.1 km have been used for studies of trypanosomiasis, East Coast fever, and malaria (Rogers and Randolph 1991, 739-41; Perry et al. 1990, 100-04).

Landsat TM, a sensor found on Landsat 4 and 5, records in the visible, reflective-infrared, mid-infrared, and thermal regions. Bands 1 through 5 and band 7 have a resolution of 30m x 30m, with the thermal infrared band 6 having a resolution of 120m x 120m. For Landsat 7, the thermal infrared band has a resolution of 60m. These bands were chosen for their use in discrimination of vegetation type and cover, soil moisture penetration, differentiation of clouds, snow, and ice, and water penetration (Jensen 2007, 203-09).

Band 4, the near-infrared band, senses in a spectral region that is sensitive to vegetation varieties and conditions (Quinn 2001). This band is useful for land/water contrasts and amount of vegetation present. Because water is a strong absorber in the near IR range, band 4 can help delineate water bodies, and discriminate between dry and moist soils, such as between barren lands and croplands (Quinn 2001). Band 4 is also important in calculating the NDVI.

Band 5, the mid-infrared band, is sensitive to water and provides detailed information about soil moisture. It also is sensitive to turgidity of water in plants (Quinn 2001). Band 5 is able to differentiate water bodies from croplands, barren lands, and

grasslands. Additionally, inland lakes and streams can be identified with greater precision using the infrared bands because of the infrared absorption of water.

The thermal band measures the radiant energy from the surface and can be used for vegetation classification, soil moisture studies, and differences in topography (Jensen 2007, 205). Determining the changes in surface temperature over time can elucidate regarding the persistence or evaporation of water ponds as a result of rainfall. Relative land surface temperatures can also be used to determine whether optimal or deterring conditions exist for mosquito development.

Remote sensing values can also be interpreted into indices using multiple band analysis. The normalized difference vegetation index (NDVI) is an index that provides a standardized method of comparing vegetation greenness and relative biomass between satellite images (Boone et al. 2000, 737-44, Chen and Brutsaert 1998, 1225-38). It is calculated as the normalized ratio of near-infrared and red and wavelength reflectance (Tucker and Townshend 1985, 369-75). Recent studies have used NDVI derived from Landsat TM imagery to determine impacts of hurricanes on forested areas, coastal vegetation, and wetlands (Rodgers, Murrah, and Cooke 2009, 496; Sheikh 2006, Ramsey et al. 2001, 279-92).

CHAPTER TWO

Methods

El Niño Southern Oscillation and hurricane activity

In order to determine the role that large-scale climate shifts may have on hurricane activity, the influence of the El Niño Southern Oscillation (ENSO) must be considered. Studies have shown that the Southern Oscillation Index (SOI) values are a primary indicator of the El Niño and La Niña cycles, which make up the ENSO (Glantz et al. 1991, 1-12; Chagas and Puppi 1986, 1-15). The SOI is calculated as a standardized difference between air pressure deviations taken at Tahiti and at Darwin, Australia (Climate Prediction Center 2009).

$$SOI = \frac{(\text{Standardized Tahiti} - \text{Standardized Darwin})}{MSD} \quad \text{eq. 1}$$

where the MSD is the monthly standard deviation. In order to solve for the SOI, the standardized Tahiti is calculated in the following way:

$$\text{Standardized Tahiti} = \frac{(\text{Actual SLP}_T - \text{Mean SLP}_T)}{\sigma_T} \quad \text{eq. 2}$$

where SLP_T is the sea level pressure at Tahiti and σ_T is the standard deviation of those pressures. Similarly, the equation for the Standardized Darwin pressure is:

$$\text{Standardized Darwin} = \frac{(\text{Actual SLP}_D - \text{Mean SLP}_D)}{\sigma_D} \quad \text{eq. 3}$$

where the SLP_D is the sea level pressure at Darwin and the σ_D is the corresponding standard deviation. To solve for the Monthly Standard Deviation (MSD):

$$MSD = \sqrt{\frac{\sum ((\text{Standardized Tahiti} - \text{Standardized Darwin}) * 2)}{N}} \quad \text{eq. 4}$$

where N is equal to the total number of summed months. The NOAA Climate Prediction Center reports SOI values on a monthly scale. SOI values were obtained for the time period of 1985 to 2007.

Using the NOAA National Hurricane Center Archive of Hurricane Seasons (www.nhc.noaa.gov), a record was obtained of all storms during the Atlantic hurricane season from 1985 to 2007. A subset of storms that impacted the Yucatan Peninsula was created from the larger Atlantic hurricane database. The databases included dates of persistence and strength based on the Saffir-Simpson scale of each hurricane. This database was analyzed and the annual numbers of hurricanes and the average intensity of the hurricanes based on the Saffir-Simpson scale were calculated. These analyses were applied separately by location (all Atlantic storms compared to storms that hit the Yucatan peninsula), and also by intensity (inclusion and exclusion of tropical storms from within the Atlantic storms and Yucatan storms). All statistical analysis was conducted in SPSS (SPSS Inc. Chicago, Il).

A Mann-Whitney *U* test was chosen in order to evaluate the difference in hurricane attributes between El Niño and La Niña cycles. El Niño and La Niña cycles were determined by evaluating the annual SOI values. Generally, years in which the SOI value is above 0.0 are considered La Niña years, whereas years in which the SOI falls below 0.0 are considered El Niño years. However, graphical representation of hurricane frequency against SOI values demonstrated a cutoff point below which the variability in hurricane frequency dropped to near zero, and above which hurricane frequency variability increased dramatically. For Atlantic storms, the SOI cutoff point was -1.02

(Fig. 1). For Yucatan storms, the SOI cutoff point was -0.90 (Fig. 2). These cutoff points were used as the bases of ranking rather than the traditional 0.00.

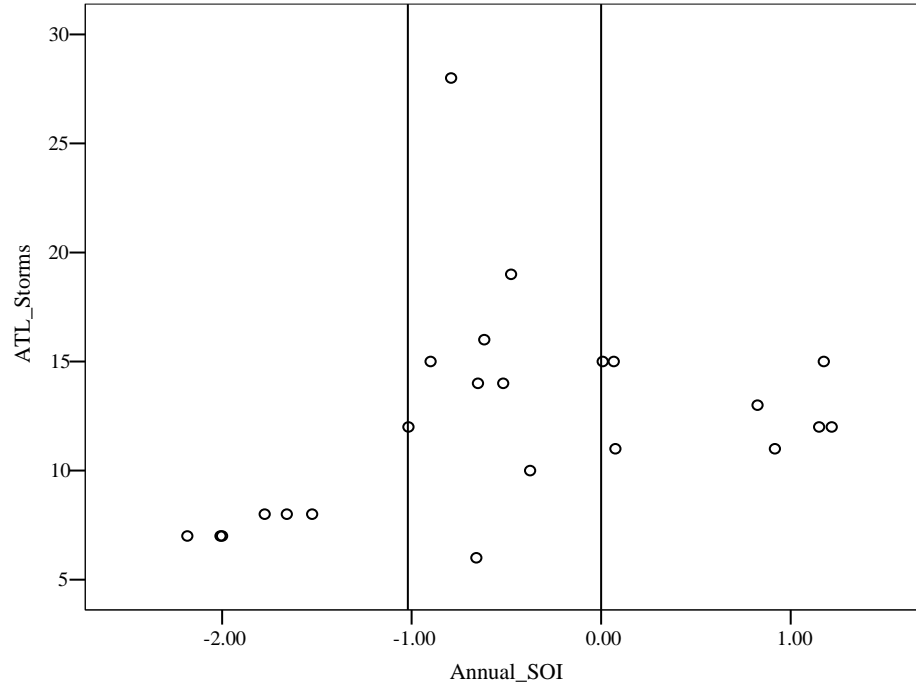


Figure 3. Distribution of Atlantic storm frequency against Southern Oscillation Index (SOI) values. Lines serve as delineations at the traditional cutoff point of 0.00 and the inferred cutoff point of -1.02, chosen due to the change in variability in storms above and below this point.

Based on the average SOI value for a given year, that year was ranked as either a “1” (indicating annual $\text{SOI} \leq \text{cutoff}$) or a “2” (indicating annual $\text{SOI} > \text{cutoff}$). The Mann-Whitney U test was run for four different outcomes; all Atlantic storms, only Atlantic hurricanes, all Yucatan storms, and only Yucatan hurricanes. Mann-Whitney U tests were also run around the same predicted cutoff value to rank the strength of hurricanes as measured by the Saffir-Simpson scale. Independent samples T-tests were run in order to determine whether a statistically significant SOI value existed as a “predictor” value around which the frequency and intensity of future hurricane seasons could be calculated.

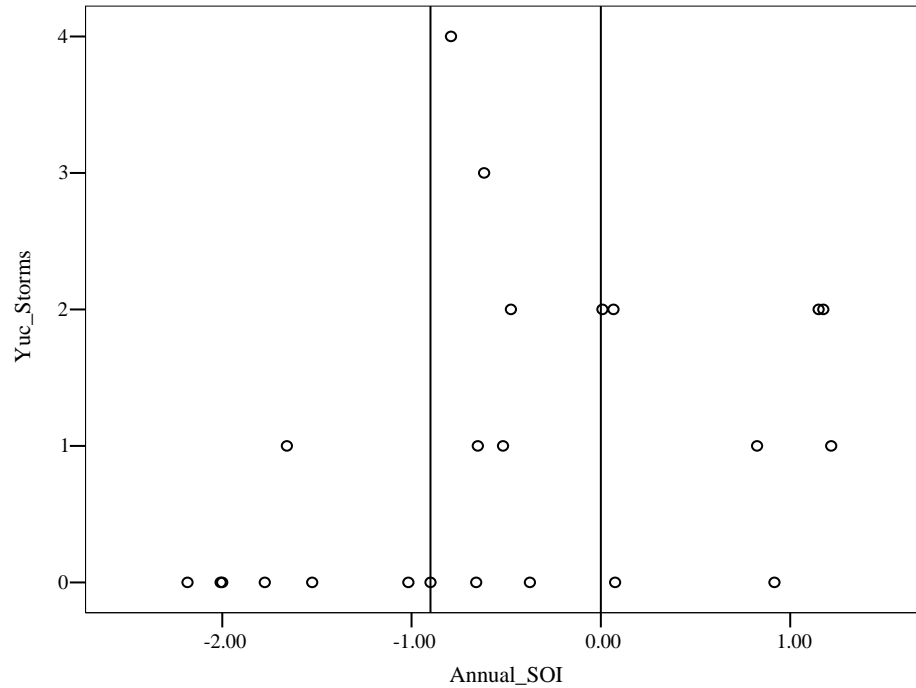


Figure 4. Distribution of Yucatan storm frequency against Southern Oscillation Index (SOI) values. Lines serve as delineations at the traditional cutoff point of 0.0 and the inferred cutoff point of -0.90. , chosen due to the change in variability in storms above and below this point.

Hurricane Impacts Detected Through Satellite Analysis

Image Selection

In order to determine land cover changes in the country of Belize, Landsat satellite data were used for satellite analysis. Using Landsat satellite data had several advantages over other satellite imagery. First, Landsat is one of the most widely used remotely sensed data because of its low cost. Numerous studies have used Landsat data to investigate changes in land cover following hurricanes (Rodgers, Murrah, and Cooke 2009, 496). Secondly, the Landsat satellites have a sun-synchronous orbit that completes a cycle around the Earth every 16 days. This provides data frequently, and due to unexpected longevity of the sensors has provided data for long periods of time.

However, the orbits do limit the Landsat data to only dates when passes are made over the study area, regardless of the extent of cloud cover. As a result, some images have a lower number of pixels that can be analyzed because of the high amount of cloud cover across the country. The temporal scale can also affect the analysis, if the dates of the orbit are not as precisely near to the hurricane event. Thirdly, the spectral resolution of sensors found on Landsat satellites is conducive to land change studies. The Thematic Mapper (TM) sensor found on Landsat satellites 4 and 5 has seven bands, from the visible through the thermal regions. The reflective bands (bands 1, 2, 3, 4, 5, and 7) have a spatial resolution of 30m, with the thermal band 6 having a resolution of 120m. The Enhanced Thematic Mapper Plus (ETM+) sensor on Landsat 7 has a similar spectral resolution, with the same seven bands, and an additional eighth band as a panchromatic band. The spectral extent of the bands on Landsat 5 and Landsat 7 are included in tables 6 and 7.

Table 6. Spectral extent of the Landsat 5 TM sensor

TM Sensor	Wavelength (μm)	Resolution (m)
Band 1	0.45 – 0.52	30
Band 2	0.52 – 0.60	30
Band 3	0.63 – 0.69	30
Band 4	0.76 – 0.90	30
Band 5	1.55 – 1.75	30
Band 6	10.40 – 12.50	120
Band 7	2.08 – 2.35	30

Source: USGS, 2009

The spectral extent of the satellites can be used to determine specific hurricane impacts on Belize. Water bodies tend to reflect highly in the visible spectrum (0.45 μm – 0.69 μm). Water bodies also increasingly absorb near and mid-infrared wavelengths (0.74 μm – 1.75 μm), making them appear darker in those images.

Vegetation conditions and soil moisture can also be differentiated by the near and mid-infrared regions.

Table 7. Spectral extent of the Landsat 7 ETM+ sensor

TM Sensor	Wavelength (μm)	Resolution (m)
Band 1	0.45 – 0.52	30
Band 2	0.53 – 0.61	30
Band 3	0.63 – 0.69	30
Band 4	0.75 – 0.90	30
Band 5	1.55 – 1.75	30
Band 6	10.40 – 12.50	60
Band 7	2.09 – 2.35	30
Band 8 (Panchromatic)	0.52 – 0.90	15

Source: USGS, 2009

Additionally, the thermal band on the ETM sensor has a resolution of 60m, and the panchromatic band as resolution of 15m. Lastly, the spatial resolution is advantageous because of the small amount of land area that is being analyzed. The country of Belize covers approximately 23,000 square kilometers (Central Statistics Office 2004). A larger spatial resolution would not be as precise in measuring land cover changes. The visible bands, near-infrared (NIR), mid-infrared (MIR), and thermal bands have all demonstrated proficiency when used to assess land cover changes. The visible and near-infrared bands can be used to determine locations of vegetation cover changes. The mid-infrared band is sensitive to water and is able to differentiate areas that have water deposition. The thermal band can be used to determine changes in surface temperature before and after the occurrence of hurricanes. Changes in temperature can indicate areas of water deposition, since areas with flooding will demonstrate a lower thermal emission than areas of dry land. Analyzing the thermal band (10.40 μm – 12.5

μm) using images taken after the hurricane and one month later can therefore show areas of persistent water deposition to supplement data from the mid-infrared band.

Landsat images were obtained from the USGS Global Visualization Viewer (usgs.glovis.gov) for the time period 1995 to 2007. For each hurricane that impacted the Yucatan Peninsula, three images were downloaded. These images correspond to three time periods under study; immediately before the hurricane, immediately following the hurricane, and one month after the hurricane. This was done in order to determine direct and persistent changes in land cover, continuous water deposition, and effects on land surface temperature. Table 8 gives a summary of the database of imagery collected for each hurricane.

Image Processing

All image processing was performed using IMAGINE 9.3 (Leica Geosystems Atlanta, GA), a software tool designed specifically to process geospatial satellite imagery. The images were acquired from Landsat 5 TM and Landsat 7 ETM.

The three scenes that comprise the country of Belize (taken from Landsat path 19, rows 47, 48 and 49) were combined to provide a single dataset for analysis. All images were georeferenced to the World WGS 1984 North, Zone 16 reference coordinate system in order to analyze them on the same spatial scale. WGS84 was used because it is a reference frame for the broadcast orbits defined by the National Geospatial-Intelligence Agency and is also closely aligned to International Earth Rotation Service Terrestrial Reference Frame (National Geodetic Survey 2009).

Table 8. Record of downloaded satellite imagery

Hurricane dates	Hurricane	Pre-hurricane	Post-hurricane	One month after
Sept. 27-Oct. 6, 1995	Opal	09-23-1995	10-09-1995	11-10-1995
Oct. 7-21, 1995	Roxanne	09-23-1995	10-25-1995	11-26-1995
Aug 19-25, 1996	Dolly	08-08-1996	08-24-1996	09-25-1996
Oct. 22-Nov. 9, 1998	Mitch	10-17-1998	11-18-1998	12-04-1998
Oct. 28-Nov 1, 1999	Katrina	10-20-1999	11-05-1999	12-07-1999
Sept. 14-21, 2000	Gordon	09-04-2000	09-20-2000	10-22-2000
Sept. 28-Oct. 6, 2000	Keith	09-20-2000	10-06-2000	10-22-2000
Aug 14-22, 2001	Chantal	06-11-2001	08-30-2001	09-15-2001
Oct. 4-9, 2001	Iris	10-01-2001	10-17-2001	01-05-2002
June 28-July 3, 2003	Bill	05-16-2003	07-19-2003	08-04-2003
July 7-17, 2003	Claudette	07-19-2003	08-04-2003	08-20-2003
Sept. 27-Oct 7, 2003	Larry	09-21-2003	10-23-2003	11-24-2003
July 3-11, 2005	Cindy	06-06-2005	07-24-2005	08-09-2005
July 11-21, 2005	Emily	06-06-2005	07-24-2005	08-25-2005
Oct. 1-5, 2005	Stan	09-10-2005	10-12-2005	11-13-2005
Oct. 15-26, 2005	Wilma	09-10-2005	10-28-2005	11-29-2005
Aug. 13-23, 2007	Dean	07-30-2007	08-31-2007	10-18-2007
Aug. 31-Sept. 6, 2007	Felix	07-30-2007	10-18-2007	11-03-2007

A shapefile of the country boundary of Belize was obtained from the Biodiversity and Environmental Resource Data System of Belize and was used to subset the satellite data for the area of Belize. Prior to any image differencing, a mask was created to exclude non-terrestrial areas (open water, cloud cover). This mask was created by using the three satellite images per hurricane as inputs to prevent inclusion of false pixel values (specifically those pixels which correlated to the Caribbean Sea and cloud cover within the country). In order to create this mask, an “if-then” equation was established to differentiate between acceptable and unacceptable pixels. This statement stated that any pixel with a value less than or equal to 0 would be classified as a “0” value and any other pixel would be classified as a “1” value.

After the masks were imposed on each image, the Normalized Difference Vegetation Index (NDVI) was calculated for each image. The NDVI was calculated using the equation:

$$NDVI = \frac{(\text{Band 4} - \text{Band 3})}{(\text{Band 4} + \text{Band 3})} \quad \text{eq. 5}$$

After the NDVI was found, calculations were run in order to determine the percent change between two consecutive images. The general equation for these calculations was as follows:

$$\text{Percent change} = 100 \times \frac{(\text{Image}_2 - \text{Image}_1)}{\text{Image}_1} \quad \text{eq. 6}$$

These calculations yielded two images; one that showed the difference between impacts immediately after the hurricane relative to conditions before the hurricane, and one that showed the difference between one month after the hurricane from the image immediately after the hurricane. The percent differences were then determined for the NDVI, the mid-infrared range, and the thermal range. The mean, standard deviation, and mode for each percent difference was calculated for NDVI, the mid-infrared range (MIR), and the thermal range (TIR). Because of the large variations in values and high standard deviations, the mode was used as the primary indicator of change rather than the mean.

Disease and Satellite Analysis

Disease epidemiological data was acquired from the Belize Ministry of Health (Epidemiology Unit 2008; Epidemiology Unit 2007; Epidemiology Unit 2006; Epidemiology Unit 2004). This data included the number of reported cases of malaria and dengue fever between the years of 1995 and 2007 (Table 9). Malaria and dengue

were chosen because they are two prevalent vector-borne diseases in the country. They also demonstrate variability annually. Epidemiological records also exist and were accessible for the time period of the study. In order to better understand the role that vegetation cover and development has on the impacts of hurricanes and the incidence of disease, a district-based analysis was also conducted. For this analysis, malaria and dengue fever epidemiological data was obtained by district from 1999 to 2007 (tables 10 and 11; Epidemiology Unit 2008).

The accuracy of the epidemiological data is an unavoidable weakness within the study. Epidemiological statistics were taken from the Belize Ministry of Health; therefore, there is no way to determine the precision with which disease reporting was completed. Currently, disease reporting is dependent on different medical facilities within a district to report to that district's health department. Those departments then report to the central Ministry of Health. This, however, leaves large room for error. For one, due to the unequal poverty levels and sparse medical facilities in Belize, and because malaria and dengue fever are endemic to the country, there is no guarantee that all people with malaria or dengue infections go to physicians for medical treatment. There is also no way to determine the accuracy of diagnosis of these diseases once someone does visit a hospital. Serotyping is done to a limited degree within the country, which reduces the accuracy of diagnosis. This can then increase the chances of both false positives and false negatives within the disease data.

Table 9. Number of malaria and dengue fever cases for the country of Belize by year

Year	Malaria	Dengue fever
1995	9413	107
1996	6605	0
1997	4014	201
1998	1936	18
1999	1853	7
2000	1486	4
2001	1092	4
2002	1113	41
2003	1319	18
2004	1066	41
2005	1549	652
2006	844	11
2007	845	63

Source: Epidemiology Unit, Ministry of Health, 2008

Table 10. Number of malaria cases by district for the country of Belize by year

Year	Belize	Stann Creek	Toledo
1999	44	307	1077
2000	26	370	632
2001	13	266	536
2002	21	268	441
2003	30	479	418
2004	24	307	303
2005	31	653	358
2006	8	405	273
2007	13	263	436

Source: Epidemiology Unit, Ministry of Health, 2008

Table 11. Number of dengue fever cases by district for the country of Belize by year

Year	Belize	Stann Creek	Toledo
1999	4	3	0
2000	4	0	0
2001	0	4	0
2002	22	0	0
2003	0	0	0
2004	13	0	13
2005	18	5	1
2006	8	0	0
2007	38	7	0

Source: Epidemiology Unit, Ministry of Health, 2008

Analysis between satellite-detected changes and disease incidence was based solely on a conceptual model that ignored socioeconomic factors, and considered only the physical characteristics that would relate to disease. The average changes in NDVI, MIR, and TIR for each year for each difference image (immediately following the hurricane – before the hurricane; one month following the hurricane – immediately following the hurricane) were compared to that year's reported incidence rates for malaria and dengue separately. In this analysis, the relationship was between the changes in NDVI, MIR reflectance, TIR emission in one year and that year's reported cases of disease. All statistical analysis was conducted in SPSS (SPSS Inc. Chicago, IL).

The percent change calculations for the NDVI, mid-infrared (MIR), and thermal infrared (TIR) bands were compared to malaria and dengue cases. Because the epidemiological data was reported on an annual time scale, it was necessary to determine the changes in NDVI, MIR and TIR also on an annual time scale. This was done by averaging the percent changes from all hurricanes within a year (for example, averaging calculated changes between hurricanes Opal and Roxanne for 1995). This was done on the assumption that the development time necessary for mosquito growth and disease transmission was confined to within that year. Using a linear regression model, the coefficient of determination was calculated comparing the diseases (malaria and dengue fever) to each calculated change (NDVI, MIR, and TIR). In order to account for multiple land use changes, multiple linear regressions were also run, comparing disease to the immediate impacts of hurricanes across the three satellite indices. This was to assess the interactions of the satellite indices. A stepwise linear regression with an F-value entry of values greater than or equal to 3.84 and removal of values less than or equal to 2.71 was

also run on the data in order to determine the model which best fit the malaria and dengue data.

The changes in NDVI, MIR, and TIR were also compared on a delayed one-year scale. This was done to determine if a lag existed as a result of mosquito development and disease transmission. The changes in NDVI, MIR, and TIR for each year for each difference image were plotted against the following year's malaria and dengue incidence rates. The correlation coefficient was calculated for each of these to determine the strength of the relationship between the changes and the disease.

Because of the disparities between the incidences of malaria and dengue within the different districts of Belize, a district-based analysis was also completed in order to determine whether hurricane impacts would affect disease incidence for areas with different land uses and development. A shapefile of Belize districts was produced by creating a JPEG file by scanning in a map of Belize (Epidemiology Unit 2008), converting it to an image file, and georeferencing the image to the WGS84 projection used for all other images. This file was then used to create areas of interest shapefiles for the districts of Belize, Stann Creek, and Toledo.

In order to determine the impact to each district, the districts were subset from hurricane images and separately analyzed through difference calculation. Using a multiple linear regression model, the coefficients of determination was calculated by comparing the diseases (malaria and dengue fever) to each calculated change (NDVI, MIR, and TIR) for each of the three districts (Belize, Stann Creek, and Toledo). Pearson correlation coefficients were also used in order to determine the degree and direction of correlations between the disease incidence and percent changes for each district.

CHAPTER THREE

Results

El Niño Southern Oscillation and Hurricane Activity

The non-parametric Mann-Whitney *U* test and independent samples T-test showed that El Niño years had significantly lower number of storms and hurricanes than La Niña for both the Atlantic and Yucatan Peninsula analyses (Table 12). For the Atlantic, during El Niño conditions, there were on average 7.50 storms, 3.50 of which were hurricanes ($p < 0.05$). However, during La Niña years, there were on average 14.00 storms, 7.82 of which were hurricanes ($p < 0.05$). For the Yucatan, El Niño conditions had on average 0.14 storms, whereas La Niña conditions had 1.31 storms ($p < 0.05$). Of those storms, 0.14 were hurricanes during El Niño conditions, and 1.06 were hurricanes during La Niña conditions ($p < 0.05$). The average Saffir-Simpson rating for Atlantic hurricanes during El Niño years was 1.90 and was 2.32 during La Niña years, although there is no significant difference between the two groups ($p > 0.05$). For Yucatan hurricanes, the average Saffir-Simpson rating was significantly different for hurricanes, with an average rating of 0.29 during El Niño years and was 1.95 during La Niña years ($p < 0.05$).

Table 12. Mann-Whitney U and independent samples T-test results for all Atlantic storms, Atlantic hurricanes only, all Yucatan storms, and Yucatan hurricanes only, ranked around a cutoff SOI values of -1.02 (for the Atlantic datasets) and -0.90 (for the Yucatan datasets). The mean rank of the two groups (with significance at $p \leq .05$), the mean frequency of storms and hurricanes (with significance at $p \leq .05$), and the average Saffir-Simpson rating for hurricanes (with significance at $p \leq .05$) for each ranked group were determined.

Model	Mean rank (SOI \leq)	Mean rank (SOI $>$)	Sig	Mean freq (SOI \leq)	Mean freq (SOI $>$)	Sig	SS rating (SOI \leq)	SS rating (SOI $>$)	Sig
Atlantic storms	4.50	14.65	0.00	7.50	14.00	0.00			
Atlantic hurricanes	4.00	14.82	0.00	3.50	7.82	0.00	1.90	2.32	0.09
Yucatan storms	7.14	14.13	0.02	0.14	1.31	0.00			
Yucatan hurricanes	7.79	13.84	0.03	0.14	1.06	0.01	0.29	1.95	0.01

Hurricane Impacts Through Satellite Analysis

The mean differences in mode from 1995 to 2007 for the NDVI, MIR, and TIR were also calculated (Table 13). Although not significantly different, analysis showed that immediately following hurricanes demonstrated an average decrease of NDVI of $-74.98 \pm 35.15\%$. The decrease in NDVI continues one month after the hurricane, with an average percent change of $-45.81 \pm 37.36\%$. Percent changes in the mid-infrared and thermal infrared ranges also decreased the two test periods, although neither the MIR nor TIR were statistically different.

Table 13: Mean differences in percent change calculations in the NDVI, MIR, and TIR from 1995 to 2007. Values shown are mean \pm standard deviation. A paired T-test determined significance at $p \leq .05$.

Satellite index	2-1	3-2	Sig
NDVI	-74.98 ± 35.15	-45.81 ± 37.36	0.11
MIR	-17.37 ± 16.71	-24.80 ± 16.99	0.33
TIR	-12.09 ± 13.21	-7.07 ± 12.49	0.37

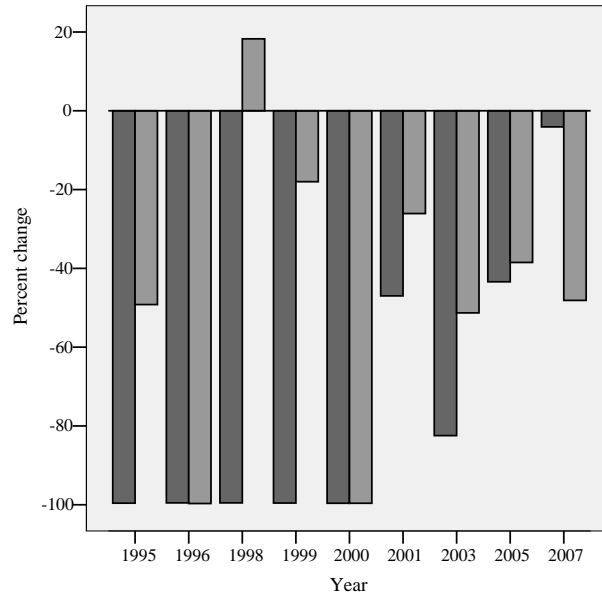


Figure 5. Percent change calculations for NDVI between images taken prior to the hurricane subtracted from images taken prior to the hurricane (dark gray) and images taken immediately after the hurricane subtracted from those taken one month after the hurricane (light gray). There is no significant difference between the two groups ($p = 0.11$).

Figure 5 illustrates the percent differences for each difference calculation for the Normalized Difference Vegetation Index (NDVI) for each year. The two groups demonstrated no statistical difference ($p > 0.05$).

Figure 6 illustrates the percent differences for each difference calculation for the mid-infrared range (MIR) for each year. The two groups demonstrated no statistical difference ($p > 0.05$).

Figure 7 illustrates the percent differences for each difference calculation for the thermal range (TIR) for each year. The two groups demonstrated no statistical difference ($p > 0.05$).

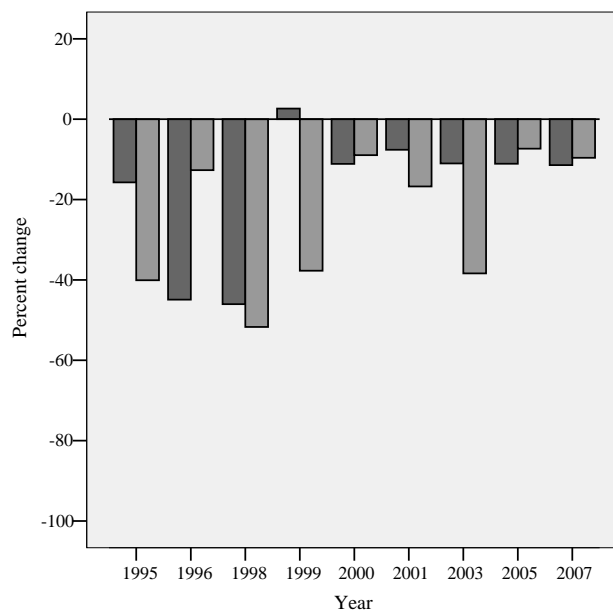


Figure 6. Percent change calculations for the MIR between images taken prior to the hurricane subtracted from images taken prior to the hurricane (dark gray) and images taken immediately after the hurricane subtracted from those taken one month after the hurricane (light gray). There is no significant difference between the two groups ($p = 0.33$).

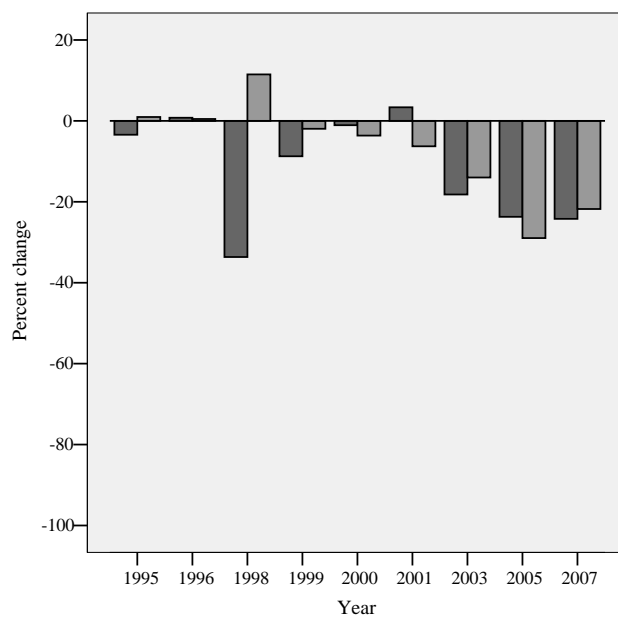


Figure 7. Percent change calculations for the TIR between images taken prior to the hurricane subtracted from images taken prior to the hurricane (dark gray) and images taken immediately after the hurricane subtracted from those taken one month after the hurricane (light gray). There is no significant difference between the two groups ($p = 0.33$).

Disease and Satellite Analysis

Country-based Analysis

Linear regression models were run in order to compare malaria and dengue fever to calculate percent changes in the NDVI, MIR, and TIR. The stepwise linear regression found that the relationship between the exponential function of the inverse of malaria and the changes in NDVI immediately after a hurricane had a significant r^2 value of 0.64 (tables 14 and 15).

Table 14. Stepwise linear regression model results comparing the relationship between the exponential function of the inverse of the incidence of malaria in Belize to percent changes in NDVI calculated between prior to a hurricane and immediately following a hurricane.

Disease	Predictors	r^2	Std. Error of estimate
Malaria	NDVI (2-1)	0.64	0.00

Table 15. ANOVA results from the stepwise linear regression of malaria and percent change in NDVI immediately after a hurricane.

Model	Sum of Squares	Df	Mean Square	F	Sig.
Regression	0.00	1	0.00	12.66	0.01
Residual	0.00	7	0.00		
Total	0.00	8			

A stepwise linear regression models run on dengue fever incidence found that the relationship between TIR one month after a hurricane was significant ($p < 0.05$) with an r^2 value of 0.51 (Tables 16 and 17).

Table 16. Stepwise linear regression model results comparing the incidence of dengue fever in Belize to percent changes in TIR calculated between immediately following a hurricane and one month after a hurricane.

Disease	Predictors	r^2	Std. Error of estimate
Dengue fever	TIR (3-2)	0.51	158.24

Table 17. ANOVA results from the stepwise linear regression of dengue fever and percent change in TIR one month after a hurricane.

Model	Sum of Squares	Df	Mean Square	F	Sig.
Regression	182459.30	1	182759.28	7.30	0.03
Residual	175288.30	7	25041.18		
Total	253047.6	8			

A stepwise linear regression analysis run taking into account a delay in mosquito development found that, for the NDVI calculations of immediately following hurricanes, the model was not significant for malaria ($r^2 = 0.47$, $p < 0.05$). For dengue fever a stepwise linear regression could not be run, but a simple linear regression found that the model was not significant between dengue fever and changes in TIR for one month after hurricane events ($r^2 = 0.01$, $p = 0.70$).

District-based Analyses

A district-based stepwise linear regression analysis was not possible because of the sample size. Also, a simple and multiple linear regression models taken for each of the districts were consistent in returning models that were not significant at the $p \leq 0.05$ value. Therefore, Pearson correlations were run to compare malaria to percent changes in NDVI (Table 18), MIR reflectance (Table 19), and TIR emittance (Table 20).

Table 18. Pearson correlation results between incidence of malaria and percent changes in the NDVI immediately after hurricanes (2-1) and one month after hurricanes (3-2) for the districts of Belize, Stann Creek, and Toledo. Significance is measured at the $p \leq 0.05$ value.

Model	NDVI 2-1 Belize	NDVI 3-2 Belize	NDVI 2-1 Stann Creek	NDVI 3-2 Stann Creek	NDVI 2-1 Toledo	NDVI 3-2 Toledo
Malaria						
Pearson Corr	-0.55	0.52	0.53	0.21	-0.48	0.38
Significance	0.26	0.29	0.28	0.69	0.33	0.46

Table 19. Pearson correlation results between incidence of malaria and percent changes in the mid-infrared (MIR) reflectance immediately after hurricanes (2-1) and one month after hurricanes (3-2) for the districts of Belize, Stann Creek, and Toledo. An asterisk (*) indicates significance at the $p \leq 0.05$ value.

Model	MIR 2-1 Belize	MIR 3-2 Belize	MIR 2-1 Stann Creek	MIR 3-2 Stann Creek	MIR 2-1 Toledo	MIR 3-2 Toledo
Malaria						
Pearson Corr	0.14	-0.59	-0.26	-0.23	0.91*	-0.17
Significance	0.79	0.22	0.63	0.67	0.01	0.75

Table 20. Pearson correlation results between incidence of malaria and percent changes in the thermal (TIR) emittance immediately after hurricanes (2-1) and one month after hurricanes (3-2) for the districts of Belize, Stann Creek, and Toledo. An asterisk (*) indicates significance at the $p \leq 0.05$ value.

Model	TIR 2-1 Belize	TIR 3-2 Belize	TIR 2-1 Stann Creek	TIR 3-2 Stann Creek	TIR 2-1 Toledo	TIR 3-2 Toledo
Malaria						
Pearson Corr	-0.93*	0.12	-0.05	-0.86*	-0.37	0.51
Significance	0.02	0.82	0.91	0.03	0.47	0.30

Pearson correlation tests found that, for malaria, the indicators that demonstrated significance were the MIR measurements taken from Toledo immediately after a hurricane ($r = 0.91$, $p < 0.05$), changes in the TIR immediately after a hurricane in Belize

district ($r = -0.93$, $p < 0.05$), and changes in the TIR one month after a hurricane in Stann Creek district ($r = -0.86$, $p < 0.05$).

Table 21. Pearson correlation results between incidence of dengue fever and percent changes in the NDVI immediately after hurricanes (2-1) and one month after hurricanes (3-2) for the districts of Belize, Stann Creek, and Toledo. Significance is measured at the $p \leq 0.05$ value.

Model	NDVI 2-1 Belize	NDVI 3-2 Belize	NDVI 2-1 Stann Creek	NDVI 3-2 Stann Creek	NDVI 2-1 Toledo	NDVI 3-2 Toledo
Dengue fever						
Pearson Corr	0.35	0.37	0.45	0.16	-0.07	-0.32
Significance	0.50	0.47	0.37	0.80	0.90	0.54

Table 22. Pearson correlation results between incidence of dengue fever and percent changes in the mid-infrared (MIR) reflectance immediately after hurricanes (2-1) and one month after hurricanes (3-2) for the districts of Belize, Stann Creek, and Toledo. Significance is measured at the $p \leq 0.05$ value.

Model	MIR 2-1 Belize	MIR 3-2 Belize	MIR 2-1 Stann Creek	MIR 3-2 Stann Creek	MIR 2-1 Toledo	MIR 3-2 Toledo
Dengue fever						
Pearson Corr	0.17	0.43	-0.48	-0.05	-0.08	0.03
Significance	0.75	0.39	0.33	0.93	0.88	0.96

Table 23. Pearson correlation results between incidence of dengue fever and percent changes in the thermal infrared (TIR) emittance immediately after hurricanes (2-1) and one month after hurricanes (3-2) for the districts of Belize, Stann Creek, and Toledo. Significance is measured at the $p \leq 0.05$ value.

Model	TIR 2-1 Belize	TIR 3-2 Belize	TIR 2-1 Stann Creek	TIR 3-2 Stann Creek	TIR 2-1 Toledo	TIR 3-2 Toledo
Dengue fever						
Pearson Corr	-0.43	-0.14	-0.51	-0.09	0.37	-0.67
Significance	0.47	0.80	0.24	0.86	0.47	0.15

Pearson correlation tests did not find any significant correlations between the incidence of dengue fever and changes in NDVI, MIR, or TIR by district for the analysis period following hurricane events (Tables 21, 22, and 23).

CHAPTER FOUR

Discussion

El Niño Southern Oscillation and Hurricane Activity

In this study, I found that hurricane activity and intensity for the Atlantic and for the Yucatan can be predicted for with statistical significance for El Niño and La Niña years, given certain SOI values. This information, in conjunction with more precise and comprehensive parameters, can be used to predict future El Niño-La Niña intensities. The El Niño Southern Oscillation (ENSO) is a consistent cyclical phenomenon that can be determined to have had historical impacts on the world climate, and will likely continue to exert increasing influence with future climate change (Boer et al. 2004; Cane 2004, 228). The influence of ENSO on increasing and decreasing the frequency and intensity of the hurricane season that impacts the Yucatan Peninsula can influence the health of the people of Belize. Therefore, more studies should assess climatic predictive factors that could be utilized to forecast hurricane impacts as a form of environmental public health prophylaxis.

The SOI measurements of air pressure deviations show a significant estimate of ENSO impacts on hurricane activity in the Atlantic. For the Atlantic, the predicted range of number of hurricanes was 7.82 and 14.0 storms for any year in which the annually averaged SOI value was above -1.02, defined as La Niña years. For years in which the SOI was below -1.02, El Niño years, the numbers of hurricanes ranged from 3.50 and 7.50. Hurricane intensities were also related to SOI values with more intense hurricanes during La Niña versus El Niño years.

My analysis also showed that the Yucatan Peninsula is impacted by hurricanes similar to the Atlantic, though with a slightly different SOI threshold value. For those years in which the SOI value was above -0.90, La Niña years, there was an average of 1.31 tropical storms and 1.06 defined hurricanes, which had an average Saffir-Simpson rating of 1.95. For those years in which the SOI was below -0.90, El Niño years, the average numbers of tropical storms and hurricanes were 0.14 and 0.14, respectively, with an average Saffir-Simpson rating of 0.29.

This analysis confirms current understanding of El Niño and La Niña conditions and their impacts on hurricane activity (Anyamba et al. 2006). El Niño conditions tend to reduce hurricane activity, while hurricane activity is expected to increase during La Niña conditions, which is confirmed by the study. Although traditionally years are separated into El Niño and La Niña conditions around the 0.00 SOI value, this study finds that analyzing at a different SOI level can also demonstrate statistically important levels of hurricane activity. This can be used to predict future hurricane seasonality and inform future researchers on the spatial variability of ENSO as a mesoscale meteorological event.

Recent studies have also attempted to predict El Niño conditions based on sea surface temperature and air pressure deviations within the Pacific (Climate Prediction Center 2009). These data indicates that, given certain parameters of air pressure deviations as measured by the SOI, future predictions of hurricane seasons in the Atlantic can be made regarding the frequency and intensity of the seasons.

The influence that the ENSO can have on specific countries such as those located on the Yucatan Peninsula reveals the type of hurricane seasons that can be expected given

SOI parameters. This type of analysis can also be adapted to address specific hazard management and mitigation policies. This foreknowledge of an intense or weak hurricane season can also contribute to early preparation for hurricane damages and resulting disease problems, not only vector-borne but also water-borne and food-borne illnesses.

Hurricane Impacts Through Satellite Analysis

Recent development and access to satellite imagery has enabled scientists to use remotely-sensed data from Landsat satellites to determine impacts of hurricanes on flooding, erosion, and changes in vegetation (Rodgers et al. 2009, David 2005). For this reason, the impacts of hurricanes were assessed through satellite analysis. Satellite analysis enabled calculations-based change detection in terms of land cover and vegetation cover changes, changes in water cover, and changes in temperature. The two time periods chosen for this study were determined to detect immediate and lasting impacts of hurricane activity. Because hurricanes can change vegetation for years following, vector habitats are also impacted. However, the specific detection of habitat qualities such as water impoundment and temperature are likely to be diluted by other environmental factors as time elapses following the hurricane disturbance.

Data calculated from Landsat-5 and Landsat-7 indicated that the impacts of hurricanes on Belize were evident for at least one month following the hurricane events. Following a hurricane, loss of vegetation (as measured by the NDVI) was substantial, and this vegetative cover loss continued one month after the hurricane, although to a lesser extent. Mid-infrared reflectance is sensitive to soil and plant moisture conditions, and can be used to differentiate between wet and dry soils (Jensen 2007, 205). This means

that MIR reflectance would decrease following the hurricane, indicating increased water presence. The decrease in MIR continued one month after the hurricane indicating areas of water inundation (Table 12). This could be because a result of increased vegetative loss, allowing for increased water ponding locations to form. Thermal infrared emittance decreased following a hurricane. This is in line with the idea that there was increasing water deposition on the surface of land areas. Water, which has a higher latent heat than soil, would tend to decrease thermal emittance. Another reason for the drop in thermal emittance is the denuding of vegetation. By removing vegetation across a certain area, the emissivity of the area decreases, causing a drop in thermal emittance (Jensen 2007, 205). The areas of water deposition continued to persist one month after the hurricane, although to a lesser extent because of evaporation. This is confirmed by the TIR measurement taken one month after the hurricane event.

The changes detected by the NDVI, MIR, and TIR were able to pick out areas that were affected by hurricanes. While this does not directly correlate to disease, understanding mosquito life cycles and habitat preferences can help determine which places are more susceptible to mosquito habitat formation. This can be important in future analysis in order to determine which land use areas (for example, agricultural, urban, or forest preserves) are more affected by hurricane activity. By understanding which areas are disproportionately affected by hurricane activity, targeted mitigation efforts can reduce or prevent epidemics.

Hurricanes demonstrate their influence through a few major indicators. Changes in vegetation following a hurricane, a result of high winds and heavy rainfall, are the most evident change that occurs. The amount of rainfall deposited during hurricanes can

then change the surface reflection in the mid-infrared range, as well as the temperature emitted from the surface. These three indicators – vegetation, mid-infrared reflection, and surface temperature changes – have shown to be the best indicators for measuring hurricane impacts on land cover changes and the resulting influence they demonstrate on mosquito populations and disease incidence. Other studies have utilized similar or the same satellite indices to determine relationships to disease incidence. Thompson et al. (1999, 2-7) studied the role that NDVI plays in predicting malaria infections in Gambia. Hay, Snow, and Rogers (1998, 13-18) studied the relationship between malaria incidence in Kenya and remotely-sensed monthly NDVI, mid-infrared (MIR) radiance data, and land surface temperature (LST). Rogers et al. (2006, 183-211) studied the role of NDVI, MIR, and LST on the incidence of dengue fever.

Disease and Satellite Analysis

Country-based Analysis

Understanding the direct and indirect impacts of hurricane activity on land cover, vegetation cover, water ponding, and surface temperature is important for assessing relationship between hurricanes and vector-borne diseases incidence. The role of hurricanes in mosquito habitat formation especially helps us to understand fluctuations in malaria and dengue fever, which are both endemic to the country of Belize. By analyzing the changes in the various satellite index values with the incidence of disease, this provided the best proximate analysis of hurricane-disease interactions.

The study found that malaria was best explained by changes occurring immediately after the hurricane rather than persistent changes caused by hurricanes. The relationship between the percent changes in NDVI immediately after a hurricane and the

inverse of the incidence of malaria demonstrated a strong correlation between vegetation removal and malaria. Whether vegetation removal leads directly to mosquito habitat formation is not clear from these results, however it does implicate disturbance of vegetation as an important feature of disease incidence.

For dengue fever, incidence was best explained by changes measured in the thermal infrared range one month after hurricanes.

The results of the regression analysis indicate that, for Anopheline mosquitoes as malarial vectors may be dependent on habitat since the strongest correlation exists between changes in NDVI. However, for Aedine species, as dengue fever vectors, is correlated to surface temperatures following disturbance. This is consistent with current understandings of the species respective life histories traits. Anopheline mosquitoes lay their eggs in shallow pools. The loss of vegetation cover, which would create new areas of ponding, as well as immediate inundation of previously dry areas, would result in an increase in *Anopheles* spp. mosquito reproduction. Aedine mosquitoes, however, are container species and can lay their eggs in dry areas. These eggs remain quiescent until the areas get inundated by rain. Temperatures cool slightly as a result of rainfall, resulting in *Aedes* larval development which was observed for most hurricane events (Fig 5).

District-based Analysis

For the analysis of satellite index changes and diseases incidence, different districts of Belize analyzed showed different sensitivities, possibly indicating variable environmental, cultural, or social factors. The Pearson correlation determined that a negative correlation existed between immediate changes in the thermal infrared emittance

and the incidence of malaria for Belize. This is explained by the temperature required for growth of mosquito larva in standing water coupled with the transience of water pools in a developing area. For Stann Creek a negative correlation existed between changes in the TIR one month after hurricane and malaria. The time difference between the Belize and Stann Creek districts is explained because there is less development and therefore likelihood of standing water to persist longer in this district. The Toledo district, however, showed a strong positive correlation between changes in mid-infrared reflectance taken immediately after a hurricane and malaria. This is a direct indicator of the presence of standing water in the area, and thus increased mosquito habitat. The lack of any significant correlation between satellite index change and dengue fever by districts is related to the low number of cases by district.

Environmental, cultural, and social issues shed light on the results of the Pearson correlation as to the differences within the districts. These factors, including vegetation cover, development, and population, have both direct and indirect impacts on disease incidence. The district of Belize has the highest level of development, higher than any of the other two districts. This helps explain the trends with disease incidence. Malaria is a disease that is commonly found in areas with high vegetation. Studies have shown that for Belize, *Anopheles* mosquitoes preferentially live in areas with forest cover and agricultural lands, because of the availability of habitat (Hakre et al. 2004). Development, with its resultant removal of natural vegetation in favor of pavement and housing areas, limits the natural habitat of the *Anopheles* mosquito.

Stann Creek exhibits a similar pattern as the district of Belize because of its increasing development. As Stann Creek moves from rural areas toward more urban

areas, increasing development affects mosquito populations. Removal of forested areas to make way for human habitation can reduce habitats for *Anopheles* mosquitoes.

The district of Toledo exhibits the behavior that one would expect from a mostly rural area. Located in the southernmost part of Belize, adjacent to Guatemala, little development has occurred in the area for a few reasons. One main reason is that the main inhabitants of the area are descendents of the Mayan Indians, who tend to live traditional agricultural lifestyles. Another reason is the success of ecotourism in the area through the promotion of a natural forests and Mayan ruins. Because of this, much of the area is still undisturbed natural vegetation. This also means ample *Anopheles* habitat and the potential for high numbers of *Aedes* mosquitoes, given rainfall.

Table 24. Percentage of population of Belize with access to sewer systems in 2004

District	Percent with access
Belize	89.6
Stann Creek	57.4
Toledo	24.8
Total country	60.8

Source: Epidemiology Unit, Ministry of Health, 2008

These results also indicate the ability of development to serve as a buffer against climatic influences. In many cases, increasing development also leads to increased sewage and drainage systems, which would have immeasurable benefits during periods of heavy rainfall (Table 24). The removal of water ponds, coupled with residual spraying around homes and buildings in developing areas, reduces the chances of mosquito vectors surviving and becoming transmitters of disease. These types of behaviors, including drainage, residual spraying, and removal of potential areas that might be susceptible to

inundation, can serve to limit Anopheline mosquito habitat and reduce the incidence of malaria within the population.

However, development can also serve as a confounding factor, affecting the relationship between disease and physical environmental characteristics. Higher population densities as a result of increased development would promote disease incidence. However, increased access to medical care, as well as preventative measures taken to reduce disease, would limit the spread of vector-borne diseases in those areas. When considering thermal emittance, increased housing for a growing population would affect the emittance of an area. By considering only environmental factors, the results of the analysis fail to consider the multiple other reasons for differences within disease incidence between districts. This study reveals that, while beneficial in some ways, in this case, analysis based solely on physical changes detected by satellites was not a good indicator for disease for the districts of Belize and Stann Creek. For Toledo, however, the limited development and high levels of forest and agricultural lands does show that physical changes can serve as a major indicator for disease.

Although correlation and regression analyses for dengue fever yielded no significant results, this does not diminish the prevalence of dengue fever in the country nor lessen the need to understand the behavior of *Aedes* mosquitoes in the transmission of the dengue virus. Considered a container species, *Aedes* mosquitoes are able to survive, and thrive, in areas with garbage collections, empty buckets, tires, and tree holes, among other places. This type of behavior indicates that Aedine species would survive better near developing or developed areas, where rainfall can result in inundation and development of mosquito larvae. This is even reflected in the raw incidence rates of

dengue fever for the different districts of Belize, Stann Creek, and Toledo (Table 11).

Although not strictly measurable by satellite analysis, actions can be taken to limit the population of *Aedes* mosquitoes, and therefore, the incidence of dengue fever, within the population through residual spraying and removal of potential habitats such as open containers, tires, and other garbage areas.

CHAPTER FIVE

Conclusions

Climate and vector-borne disease are related in some way. The sharpness of this relationship was very difficult to define in this study, however. Nevertheless, climate has been shown to have an affect on countries, regardless of size. Large-scale climatic phenomena such as the El Niño Southern Oscillation, the North Atlantic Oscillation, and the Pacific Decadal Oscillation have all demonstrated impacts world-wide. Small countries, like Belize, are exposed to the same climatic influences.

Considering this, climate change can indeed affect small countries. Aside from the changes in global surface temperature, increases in the variability of climatic phenomena can have potentially disastrous effects on small countries, which often have limited management capabilities due to their size. As globalization and urbanizing development continue world-wide, more attention needs to be given to the potential hazards this creates in an epidemiological sense.

Moderate resolution satellites, such as the Landsat, have the advantage of being both inexpensive and widely available. They have provided long-term useful data for large-scale studies. However, use of these moderate resolution satellites for studies of smaller countries is not as proficient as hoped. Although the capabilities within the satellites allow for similar tests as higher-resolution satellites, problems such as cloud cover, missing data, or sensor problems can yield meaningless results.

The use of these satellites in epidemiological capabilities is not to be underscored, however. Satellite data alone is not a good predictor of disease within countries.

However, because of the temporal resolution of the satellites, basic predictors of disease (such as changes in land surface temperature or amount of rainfall within a country in a given time period) can be determined and monitored through the use of these satellites, and can be useful in predicting and preventing future epidemics.

REFERENCES

- Achee, Nicole, John Grieco, Penny Masuoka, Richard Andre, Donald Roberts, James Thomas, Ireneo Briceno, Russell King, and Eliska Rejmankova. "Use of remote sensing and geographic information systems to predict locations of *Anopheles darlingi*-positive breeding sites within the Sibun River in Belize, Central America," *Journal of Medical Entomology*, 43 (2006): 382-392.
- Andre, Richard, Donald Roberts, and Eliska Rejmankova. "The recent application of remote sensing and geographic information system technologies to the study of malaria vector populations," *Acta Med*, 31 (1995): 27-35
- Anyamba, Assaf, Jean-Paul Chretien, Jennifer Small, Compton Tucker, and Kenneth Linthicum. "Developing global climate anomalies suggest potential disease risks for 2006-2007," *International Journal of Health Geographics*, 6 (December 2006), under "Research," <http://www.ij-healthgeographics.com/content/5/1/60> (accessed February 23, 2009).
- Bayoh, Mohamed and Steve Lindsay. "Effect of temperature on the development of the aquatic stages of *Anopheles gambiae* sensu stricto (Diptera:Culicidae)," *Bulletin of Entomological Research*, 93 (2003): 375-381.
- Biodiversity and Environmental Resource Data System of Belize. "Belize shapefile." < <http://www.biodiversity.bz/find/resource/profile.phtml?dcid=1156/> [accessed June 1, 2009].
- Boer, George, Bin Yu, S.J. Kim, and Gregory Flato. "Is there observational support for an El Niño-like pattern of future global warming?" *American Geophysical Union*, 40 (March 2004): under "Geophysical Research Letters," <http://www.cccma.ec.gc.ca/papers/gboer/PDF/Obs_ElNino.pdf> [accessed July 13, 2009].
- Boone, Randall, Kathleen Galvin, Nicole Smith, Stacy Lynn. "Generalizing El Nino effects upon Maasai livestock using hierarchical clusters of vegetation patterns," *Photogrammetric Engineering and Remote Sensing*, 66 (2000): 737-744.
- Bouma, Menno, and Hugo van der Kaay. "The El Niño Southern Oscillation and the historic malaria epidemics on the Indian subcontinent and Sri Lanka: An early warning system for future epidemics?" *Tropical Medicine and International Health*, 1 (1996): 86-96.

- Bouma, Menno and Christopher Dye. "Cycles of malaria associated with El Niño in Venezuela," *Journal of the American Medical Association*, 278 (1997): 1772-1774.
- Bunyavanich, Supinda, Christopher Landrigan, Anthony McMichael, and Paul Epstein. "The impact of climate change on child health," *Ambulatory Pediatrics*, 3 (2003): 44-52.
- Cane, Mark. "The evolution of El Niño, past and future," *Earth and Planetary Science Letters*, 230 (2005): 227-240.
- Central Statistics Office. 2004. *Environmental statistics for Belize 2004*. Belize: Ministry of National Development.
- Chagas, Christiane, and G. Puppi. *Persistent Meteo-Oceanographic Anomalies and Teleconnections*. Cite Del Vaticano, Pontificia Academia Scientiarum, 1986.
- Chaves, Luis, Justin Cohen, Mercedes Pascual, and Mark Wilson. "Social exclusion modified climate and deforestation impacts on a vector-borne disease," *PLoS Neglected Tropical Diseases*, 2 (February 2008), under "Neglected Tropical Diseases,"
<http://www.ncbi.nlm.nih.gov/pmc/articles/PMC2238711/pdf/pntd.0000176.pdf>
 [accessed June 1, 2009].
- Checkley, William, Leonardo Epstein, Robert Gilman, Dante Figueroa, Rosa Cama, and Jonathan Patz. "Effects of El Niño and ambient temperatures on hospital admissions for diarrhoeal diseases in Peruvian children," *Lancet*, 355 (2000): 442-450.
- Chen, Daoyi and Wilfried Brutsaert. "Satellite-sensed distribution and spatial patterns of vegetation parameters over a tallgrass prairie," *Journal of Atmospheric Sciences*, 55 (1998): 1225-1238.
- Climate Prediction Center. 2009. El Niño/Southern Oscillation (ENSO) Diagnostic Discussion. Camp Springs, Maryland: NOAA/National Weather Service.
- Climate Prediction Center. "How is the SOI calculated?"
<http://www.cpc.noaa.gov/data/indices/Readme.index.shtml#SOICALC/> [accessed February 20, 2009].
- el-Akad, Adel. "Effect of larval breeding conditions on the morphological, ovarian, and behavioral characteristics of *Anopheles pharoensis* of the merged females," *Journal of Egyptian Society of Parasitology*, 21 (1991): 459-465.
- Epidemiology Unit. 2008. *Belize Basic Indicators 2007 Volume 5*. Ministry of Health, Belize.

- Epidemiology Unit. 2007. *Belize Basic Indicators 2006 Volume 4*. Ministry of Health, Belize.
- Epidemiology Unit. 2006. *Belize Basic Indicators 2005 Volume 3*. Ministry of Health, Belize.
- Epidemiology Unit. 2004. *Belize Basic Indicators 2003 Volume 1*. Ministry of Health and Communication, Belize.
- Epstein, Paul. "Climate and health," *Science*, 285 (1999): 347-348.
- Epstein, Paul. "Climate change and emerging infectious diseases," *Microbes and Infection*, 3 (2001): 747-754.
- Epstein, Paul. "Climate change and infectious diseases: stormy weather ahead," *Epidemiology*, 13 (2002): 373-375.
- Epstein, Paul. "Climate change and human health," *The New England Journal of Medicine*, 353 (2005): 1433-1436.
- Foster, Woodbridge and Edward Walker. Mosquitoes (*Culicidae*). *Medical and Veterinary Entomology*. California: Academic Press, 2002.
- Gabaldon, Arnoldo. "A nation-wide campaign against malaria in Venezuela," *Transactions of the Royal Society of Tropical Medicine and Hygiene*, 43 (1949): 113-132.
- Glantz, Michael, Richard Katz, and Neville Nicholls. *Teleconnections Linking World Wide Climate Anomalies: Scientific Basis and Societal Impact*. New York: Cambridge University, 1991.
- Grieco, John, Sarah Johnson, Nicole Achee, Penny Masuoka, K. Pope, Eliska Rejmankova, Erol Vanzie, Richard Andre, and Donard Roberts. "Distribution of *Anopheles albimanus*, *Anopheles vestitipennis*, and *Anopheles crucians* associated with land use in northern Belize," *Journal of Medical Entomology*, 43 (2006): 614-622.
- Guerra, Carlos, Robert Snow, and Simon Hay. "A global assessment of closed forests, deforestation, and malaria risk," *Annals of Tropical Medicine and Parasitology*, 100 (2000): 189-204.
- Hakre, Shilpa, Penny Masuoka, Erol Vanzie, and Donald Roberts. "Spatial correlations of mapped malaria rates with environmental factors in Belize, Central America," *International Journal of Health Geographics*, 3 (March 2004), under "Research," <http://www.ij-healthgeographics.com/content/3/1/6> (accessed February 23, 2009).

- Haworth, Jean. "The global distribution of malaria and the present control effort," *Malaria: Principles and Practice of Malariology*, Edinburgh: Churchill Livingstone, 1988.
- Hay, Simon. "Remote sensing and disease control: Past, present, and future," *Transactions of the Royal Society for Tropical Medicine and Hygiene*. 91 (1997): 105-106.
- Hay, Simon, Robert Snow, and David Rogers. "Predicting malaria seasons in Kenya using multitemporal meteorological satellite sensor data," *Transactions of the Royal Society for Tropical Medicine and Hygiene*. 92 (1998): 12-20.
- Hood, Susan. *Hurricanes*. New York: Simon Spotlight, 1998.
- Hugh-Jones, Martin. "Applications of remote sensing to the identification of habitats of parasites and disease vectors," *Parasitology Today*, 5 (1989): 244-251.
- Jensen, John, James Campbell, Jeff Dozier, James Estes, Michael Hodgson, C.P. Lo, Kamlesh Lulla, James Merchant, R. Smith, Douglas Stow, Arthur Strahler, and Rodney Welch. Remote sensing. *Geography in America*. Columbus, OH, Merrill, 1989.
- Jensen, John. *Remote sensing of the environment*. New Jersey: Pearson Prentice Hall, 2007.
- Khasnis, Atul and Mary Nettleman. "Global warming and infectious disease," *Archives of Medical Research*, 36 (2005): 689-696.
- Kitron, Uriel and Alessandro Mannelli. "Modelling the ecological dynamics of tick borne zoonoses," *Ecological dynamics of tick-borne zoonoses*, New York: Oxford University Press, 1994.
- Kitron, Uriel. "Landscape ecology and epidemiology of vector-borne diseases: Tools for spatial analysis," *Journal of Medical Entomology*, 35 (1998): 435-445.
- Kurane, Ichiro. "Dengue hemorrhagic fever with special emphasis on immunopathogenesis," *Comparative Immunology, Microbiology, and Infectious Diseases*. 30 (2006): 329-340.
- Land and Surveys Department. 2006. *Our environment in figures 2006*. Belize: Ministry of Natural Resources and the Environment.
- Lillesand, Thomas and Ralph Kiefer. *Remote sensing and image interpretation*. New York: Wiley, 1994.

- Lindblade, Kim, Edward Walker, Ambrose Onapa, Justus Katungu, and Mark Wilson. "Land use change alters malaria transmission parameters by modifying temperature in a highland area of Uganda," *Tropical Medicine and International Health*, 5 (2000): 263-274.
- Lindsay, Steve and Willem Martens. "Malaria on the African highlands: past, present, and future," *Bulletin of the World Health Organization*, 76 (1998): 33-45.
- Linthicum, Kenneth, Charles Bailey, F. G. Davies, and Compton Tucker. "Detection of Rift Valley fever viral activity in Kenya by satellite remote sensing imagery," *Science*, 235 (1987): 1656-1659.
- Linthicum, Kenneth, Charles Bailey, Compton Tucker, D.R. Angleberger, Terry Cannon, Timothy Logan, Paul Gibbs, and Jaime Nickeson. "Towards real-time prediction of Rift Valley fever epidemics in Africa," *Preventative Veterinary Medicine*, 11 (1991): 325-334.
- Linthicum, Kenneth, Assaf Anyamba, Compton Tucker, Patrick Kelley, Monica Myers, and Clarence Peters. "Climate and satellite indicators to forecast Rift Valley fever epidemics in Kenya," *Science*, 285 (1999): 397-400.
- Macdonald, George. *The Epidemiology and Control of Malaria*. London: Oxford University Press, 1957.
- Monath, Thomas. *Arboviruses: Epidemiology and ecology*. Boca Raton, Florida, CRC Press, 1988.
- NASA, "NASA Study Predicted Outbreak of Deadly Virus." *ScienceDaily* (Feb. 2009), <http://www.sciencedaily.com/releases/2009/02/090217101433.htm> [accessed October 15, 2009].
- National Geodetic Survey. "Frequently Asked Questions." < <http://www.ngs.noaa.gov/faq.shtml#WGS84> > [accessed June 15, 2009].
- National Oceanic and Atmospheric Administration. "National Hurricane Center Archive of Hurricanes." <http://www.nhc.noaa.gov/pastall.shtml/> [accessed February 20, 2009].
- National Policy Development Committee. 2003. *Belize National Hazard Mitigation Policy Third Draft*. Belize.
- Nicholls, Neville. "A method for predicting Murray Valley encephalitis in southeast Australia using the Southern Oscillation," *Australian Journal of Experimental Biology and Medical Science*, 64 (1986): 587-594.

- Nicholls, Neville. "El Niño-Southern Oscillation and vector-borne disease," *Lancet*, 342 (1993): 1284-1285.
- Palsson, Katinka, Thomas Jaenson, Francisco Dias, Anne Laugen, and Anders Bjorkman. "Endophilic *Anopheles* mosquitoes in Guinea Bissau, West Africa, in relation to human housing conditions," *Journal of Medical Entomology*, 41 (2004): 746-752.
- Pascual, Mercedes, Xavier Rodo, Stephen Ellner, Rita Colwell, and Menno Bouma. "Cholera dynamics and El Niño -Southern Oscillation," *Science*, 289 (2000): 1766-1769.
- Patz, Jonathan and William Reisen. "Immunology, climate change, and vector-borne diseases," *Trends in Immunology*, 22 (2001): 171-172.
- Perry, Billie, Paul Lessard, R.A.I. Norval, K. Kundert, and Russ Kruska. "Climate, vegetation and the distribution of *Rhipicephalus appendiculatus* in Africa," *Parasitology Today*, 6 (1990): 100-104.
- Pulwarty, Roger. "Annual and interannual variability of convection over tropical South America" PhD thesis, Department of Geography, University of Colorado, Boulder, Colorado, USA, 1994.
- Quinn, Jeffrey. 2001. "Landsat band combinations." <http://web.pdx.edu/~emch/ip1/band combinations.html/> [accessed July 29, 2009].
- Ramsey, Elijah III, Michael Hodgson, Sijan Sapkota, and Gene Nelson. "Forest impact estimated with NOAA AVHRR and Landsat TM data related to an empirical hurricane wind-field distribution," *Remote Sensing of Environment*, 77 (2001): 279-292.
- Rodgers, John III, Adam Murrah, and William Cooke. "The impact of Hurricane Katrina on the coastal vegetation of the Weeks Bay Reserve, Alabama from NDVI data," *Estuaries and Coasts*, 32 (2009): 496-507.
- Rogers, David and Sarah Randolph. "Mortality rates and population density of tsetse flies correlated with satellite imagery," *Nature* 351 (1991): 739-741.
- Rogers, David, A.J. Wilson, Simon Hay, and A.J. Graham. "The Global Distribution of Yellow Fever and Dengue," *Advances in Parasitology*, 62 (2006): 181-220.
- Sheikh, Pervaze. "The Impact of Hurricane Katrina on biological resources," CRS Report for Congress. The Library of Congress, 2006.
- Statistical Institute of Belize. 2008. *Abstract of statistics 2007*. Belize: Statistical Institute of Belize.

- Steffen, Will, Angelina Sangerson, Peter Tyson, Jill Jager, Pamela Matson, Berrien Moore III, Frank Oldfield, Katherine Richardson, H. John Schellnhuber, B.L. Turner III, and Robert Wason. *Global change and the earth system*. Germany: Springer-Verlag, 2005.
- Thompson, Madeleine, Stephen Conner, Umberto D'Alessandro, Barry Rowlingson, Peter Diggle, Mark Cresswell, and Brian Greenwood. "Predicting malaria infection in Gambian children from satellite data and bed net use surveys: The importance of spatial correlation in the interpretation of results," *American Society of Tropical Medicine and Hygiene*, 61 (1999): 2-8.
- Treaster, Joseph. *Hurricane force: In the path of America's deadliest storms*. Boston: Kingfisher, 2007
- Tucker, Compton and John Townshend. "African land-cover classification using satellite data," *Science*, 227 (1985): 369-375.
- Unisys Weather. 2007. *Hurricane/Tropical data Atlantic Tropical Storm Tracking by Year*. <http://www.liu.edu/cwis/cwp/library/workshop/citapa.htm> [accessed February 20, 2009]
- United States Geological Survey. "Landsat Band Combinations." http://landsat.usgs.gov/band_designations_landsat_satellites.php/ [accessed July 12, 2009].
- Veronesi, R. 1991. *Doencas Infecciosas e Parasitarias*. Rio de Janeiro, Guanabara Koogan.
- Waddell, D.A.G. 1961. *British Honduras: A historical and contemporary survey*. New York: Oxford University Press.
- Woodruff, Rosalie, Charles Guest, Michael Garner, Niels Becker, Janette Lindesay, Terence Caravan, and Kristie Ebi. "Predicting Ross River virus epidemics from regional weather data," *Epidemiology*, 13 (2002): 384-393.
- Wyse, Ana, Luiz Bevilacqua, and Marat Rafikov. "Simulating malaria model for different treatment intensities in a variable environment." *Ecological Modelling* 206 (2007): 322-330.
- Yang, Hyun and Claudia Ferreira. "Assessing the effects of vector control on dengue transmission," *Applied Mathematics and Computations*. 198 (2007): 401-413.
- Washino, Robert and Brent Wood. "Application of remote sensing to vector arthropod surveillance and control," *American Journal of Tropical Medicine and Hygiene*, 50 (1994): 134-144.